Title: Improving X-Ray Optics Through Differential Deposition

P.I.: Brian Ramsey / Space Science Office/ ZP12/ NASA Marshall Space Flight Center
Brian.Ramsey@nasa.gov; 256-961-7784

Co.Is.:

NASA/Marshall Space Flight Center:
Kiranmayee Kilaru
Kiranmayee.Kilaru-1@nasa.gov
Mikhail Gubarev
Mikhail.V.Gubarev@nasa.gov
Jessica Gaskin
Jessica.A.Gaskin@nasa.gov
Steve O'Dell
Steve.O'Dell@nasa.gov
Jeffery Kolodziejczak
Jeff.Kolodziejczak@nasa.gov

Smithsonian Astrophysical Observatory:
Suzanne Romaine
Romaine@head.cfa.harvard.edu

GSFC:
William Zhang
William.W.Zhang@nasa.gov

University of Alabama, Huntsville:
Carolyn Atkins
ca0007@uah.edu

RFI Submitted in Response to NNH11ZDA018L: Concepts for the Next NASA X-ray Astronomy Mission

Category of Response: *Enabling Technology*

Willing to participate and present concept: *YES*

Overview of Planned Research

The key performance metrics for x-ray telescopes are angular resolution and aperture area. Due to mass constraints of space telescopes and the large ratio (about 100:1) of mirror surface area to (projected) aperture area for X-ray optics, future large-aperture x-ray telescopes require light-weight (about a kg/m^2 areal density) elements. The precision, thick-walled (about 50 kg/m^2) *Chandra X-ray Observatory* optics achieved sub-arcsecond angular resolution. In contrast, state-of-the-art light-weight mirror technologies—electroformed-nickel, slumped-glass, and silicon-pore—achieve (at best) of order 10 arcsecond angular resolution. We should emphasize that even the 10-arcsecond level of resolution has only been achieved at the sub-system level. The technological challenge is to obtain the fine angular resolution of *Chandra* with optics that are 50 times lighter.

The inherently low stiffness of large-area light-weight mirrors renders them susceptible to deformation during fabrication and mounting. Hence, obtaining substantially better angular resolution (of order an arcsecond or less) with light-weight mirrors will require a significant modification of the way mirror figure is imparted and maintained. One approach for achieving better angular resolution with light-weight mirrors is *differential* (or *selective*) *deposition*.

Differential deposition involves selectively depositing material on the mirror's surface, to correct low-to-mid-spatial-frequency errors, inherent in the fabrication process, that degrade the angular resolution of x-ray optics. The technique has already been used by other groups working with sub-arcsecond synchrotron optics, to convert cylindrical optics to elliptical form[1] and for general figure correction[2]. We have demonstrated proof-of-concept on Wolter-type full-shell x-ray optics using physical vapor deposition to correct the surface figure of miniature (few-cm scale) mirrors intended for medical imaging[3]. Here we propose to scale the process to full-shell and segmented mirrors of a size applicable to x-ray astronomy. Our simulations indicate that, given adequate metrology, this technique can substantially improve the angular resolution of x-ray optics. Unlike mechanical polishing, differential deposition is a non-contact figuring process and can be used to correct the figure of mounted, as well as unmounted, mirrors. Note that for short mirrors with small sagittal depth (such as those needed for wide-field x-ray telescopes), differential deposition is capable of figuring a cone to a prescribed axial figure.

The specific objectives of a proposed 3-year investigation are these:

1) *Design and build a coating system that will permit differential deposition correction for segmented and for full-shell astronomical x-ray optics;*
2) *Fully characterize the parameters of the completed system to determine optimal coating rates for high-quality deposits with minimal internal stresses;*
3) *Demonstrate the differential deposition technique on segmented and on full-shell astronomical x-ray optics, quantify the final performance of the optic, and identify the future research to achieve any additional improvements.*

1.1. IXO Requirements

IXO addresses a broad range of high-energy astrophysics questions. Among these are several that require high angular resolution and the associated increase in sensitivity. These include measuring the physical and chemical properties of the intergalactic medium along sight-lines to distant quasars, tracing the evolution of galaxy clusters using precise profiles of metal abundance and the thermodynamic state of clusters out to high redshift, quantifying the effects of radiative and mechanical feedback from supermassive black holes on their surrounding environments in the form of gas heating and outflows, and pinpointing the sites of shock acceleration of electrons in Galactic supernova remnants.

The IXO science requires an angular resolution of 5 arcsec or better. One of two proposed competing versions of the IXO flight mirror assembly utilized segmented glass optics. In this design[4], commercially-available glass segments are thermally slumped onto properly figured mandrels by softening the glass at high temperature. After trimming and depositing an optical coating, the slumped-glass mirrors are aligned and assembled into a Wolter type-1 (paraboloid – hyperboloid) configuration. The currently measured half-energy width of a *single* mirror pair is slightly less than 10 arcsec. The dominant contributors to the image blur are low-order axial-figure errors: mean axial sag (sagittal depth) and azimuthal variations in axial slope and axial sag. The amplitude of these errors is a few-to-several tenths micrometer (i.e., a few-to-several hundred nanometer). This is the approximate range of surface-error amplitudes that differential deposition can correct.

The two-reflection root-mean-squares (RMS) image blur is given by $\sigma_\vartheta = 2\sqrt{2}(2\pi\sigma_h / \lambda)$, where σ_h is the RMS height error for surface deviations of spatial wavelength. Now consider the last NASA IXO design, which utilized 200-mm long slumped-glass mirrors. For this length mirror, the error term corresponding to sag has a spatial wavelength of 400 mm. If the differential deposition can correct a 300-nm sag error to an accuracy 30 nm, it would reduce the contribution of the sag error to the RMS blur from about 3 arcsec to about 0.3 arcsec. Note that the maximum coating thickness (without introducing significant stresses) basically determines the capture range of this process: That is, the mirror must meet some minimum performance criterion before the differential deposition can correct it effectively. Once the mirror is in this capture range, then the accuracy of the coating deposition (and associated metrology) determines how fine an angular resolution can be achieved.

2. Differential Deposition

2.1. Overview

Differential deposition seeks to correct figure errors, imparted during fabrication and assembly, by selectively depositing a filler material on the mirror's reflective surface. To implement the technique, the actual figure profile of the mirror to be corrected is measured and compared with the desired profile. The difference between these two profiles forms an error or 'hit' map that describes the location and amount of material that must be deposited.

The correction technique is realized through the use of physical vapor deposition, with sputtering being the preferred approach due to its superior surface quality and flexibility of

target materials over conventional evaporation. Depending on the mirror material and geometry, the sputtering can be either via DC or RF activation. For either case, a mask, under computer control, is used to limit and define the extent of the deposition to correct the figure on the appropriate spatial scales.

The effectiveness of differential deposition for correcting mirror figure hinges on multiple factors that must be addressed for successful implementation. Of paramount importance is accurate metrology of sufficient resolution to determine the spatial scales and amplitudes to be corrected. Given this, then a filler material must be selected that can provide coating thicknesses of required amplitudes without increasing surface roughness or resulting in figure-distorting stresses. Finally, one must apply accurately-determined coating thicknesses over precisely-controlled areas, such that the desired figure-correcting profile is applied.

2.2. Work to Date

As a proof of concept, we have demonstrated the principles of differential deposition on miniature full-shell grazing-incidence optics, developed at MSFC for small animal radionuclide imaging[5]. These x-ray mirrors were designed for finite distance imaging and thus consist of segments of confocal elliptical and hyperbolic surfaces. The optics have a diameter of 32 mm and an overall length of 60 mm to meet the medical imaging requirements. Their angular resolution is limited by sub-micron-amplitude axial figure errors imparted by stress during the electroforming process, typical of all electroformed optics.

The experimental configuration used to perform the differential deposition on these optics is displayed schematically in Figure 1. The system consists of a metal cathode sputtering rod, a mask, and the optic to be corrected, all mounted concentrically. The mask opening is a slit with a precise width to control the spatial extent of the deposition on the shell; the slit width is chosen to correct specific spatial scale figure deviations. In order to give the best-defined coating profile and the highest rate of deposition, the slit is positioned as close to the shell as physically possible. During the deposition process the shell rotates over the mask and translates linearly with predefined variable velocity (determined from simulations) to vary the amount of material deposited and hence the deposition profile. The translation and rotation stages are both under computer control.

Radio-Frequency (RF) sputtering was used for the vacuum deposition, with the target rod connected to the RF supply. An inert gas (such as argon or xenon) provides the source of heavy ions, via the RF–induced plasma, that in turn sputter the material from the target rod.

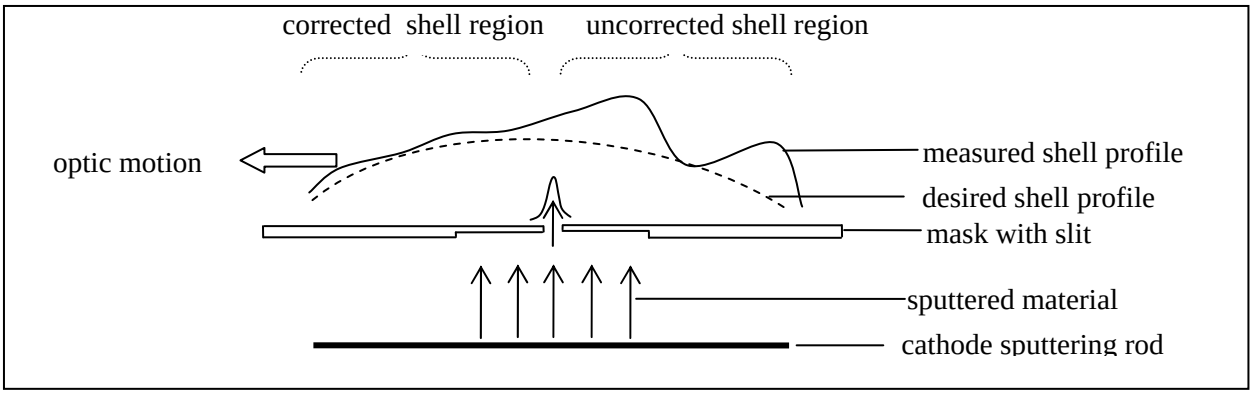

Figure 1: *Schematic of experimental configuration for differential deposition.*

The accuracy and repeatability in measuring the precise amplitude and shape of figure deviations plays an extremely important role in the implementation of this figure-correcting technique. A Form-Talysurf contact-probe profilometer was used to measure the surface axial figure profile of the small shells. To improve repeatability, the shells were held in a custom-built rigid mount and several sets of data were taken at each position and then averaged to reduce random errors in the measurement process.

Simulations also play a key role in implementing the differential deposition process. The slit size of the mask is chosen based on the size of the particular features to be corrected. Once the profile of the sputtered beam has been calibrated it can then be fit with an analytical curve. The superposition of many such curves can then be used to generate the desired profile, varying the amplitude of the curve at each position (i.e., the thickness of material deposited) to achieve the desired profile. Given the measured coating rate in the chamber, the desired amplitude can then be converted to a mask dwell time. These data then serve as the input to the computer system controlling the chamber translation stage.

The simulations were also used to determine the optimum approach to correcting the mirror shells. It was found that broad features, which were typically large amplitude, should be corrected first using relatively coarse masks, and then progressively finer features, with typically smaller amplitude deviations, should be tackled with progressively smaller mask slits. Thus several stages of correction could be needed, depending upon the desired final angular resolution.

Before shell corrections were made, suitable filler materials and coating parameters were tested. The optimum filler material has a high deposition rate, very low internal stress, high adhesion and smooth surfaces, even for thick deposits. Various filler materials, coating power, and sputtering gas type and pressure were tested until an optimum combination (xenon sputtering gas and nickel filler material) was found.

Figure 2 shows an example of the desired and actual profile using the differential deposition system. These results indicate that broad features can be successfully corrected by the differential deposition technique and gives us confidence that deposition rates can be

reliably determined, that the computer simulations are valid, and that suitable slit and velocity profiles can be determined to provide this level of correction.

Figure 2 also indicates, however, that higher frequency errors are still present and that these will now dominate the angular resolution of the improved optic. Thus the first stage of the correction process has been completed, but successive stages, which are typically higher frequency and smaller amplitude, now require more precise metrology.

The contact profilometer used at MSFC, the only instrument available to us that is capable of measuring inside these small test shells, has a repeatability of about +/- 100 nm on a single run and this is reduced to about +/- 20 nm by averaging over 20 measurements. This level of accuracy is adequate for the first stage of correction, where typical amplitudes (based on representative shells) to be corrected are a few hundred nm. The second stage of correction will require an accuracy of about 5 nm to produce any significant improvement and this is beyond the capability of this profilometer. However, more accurate non-contact profilometers are available at MSFC for use with the larger-diameter astronomical optics proposed for investigation here

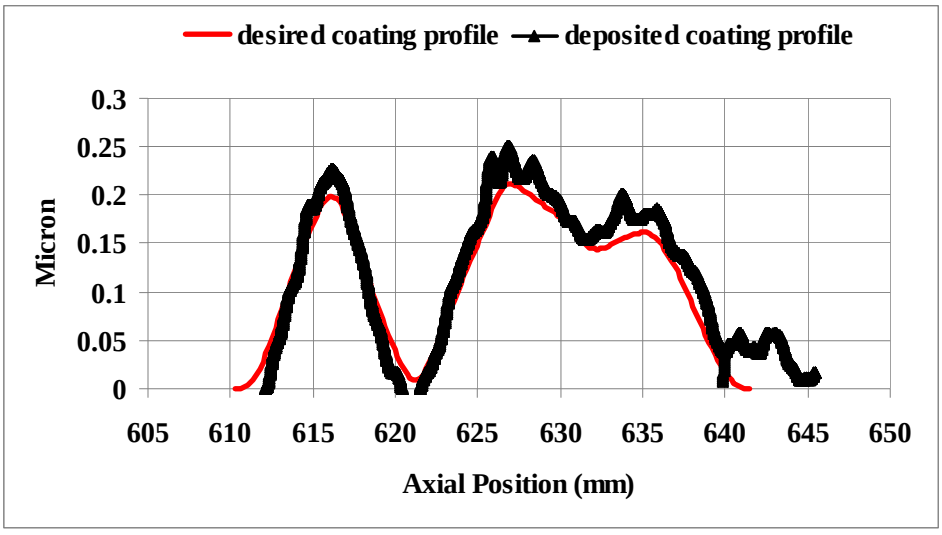

Figure 2: *Desired and measured coating profile.*

2.3. Potential of the Technique

As discussed above, the main limitation in the proof-of-concept tests performed on the small-animal-imaging optics was the inherent error in the contact profilometer that was used for shell metrology. This type of metrology was necessitated by the very small shell diameter which ruled out the use of the much-more-accurate non-contact interferometric profilometers that are typically used at MSFC for inside shell metrology of astronomical optics. We can therefore ask, what would be the limitation of the technique with improvements? Several factors contribute here. In addition to shell metrology, there are errors in registration of the mask relative to the shell, as well as uncertainties in deposition rate and actual beam profiles.

We have simulated some of these effects to get a better understanding of what may be achievable in terms of optic improvement.

To gauge the necessary profilometry accuracy, we have taken measured axial figure profiles from a 6.8 arcsec HPD full-shell astronomical optic fabricated at MSFC and applied the differential deposition technique via modeling, to derive predicted performance improvement for various stages of correction. The results of this modeling are shown below in Table 1. From these results, we see that for the full benefit of the first stage of correction, a metrology accuracy of +/- 10 nm is adequate, whereas for the second stage of correction this must improve to ~ +/- 5 nm to see any significant enhancement (ideally to +/-1 nm). For the third stage, the metrology must be progressively more accurate to realize further improvements.

Table 1: *Effects of metrology accuracy (amplitude uncertainty) on ultimate resolution for various stages of figure correction*

Correction stage	Average deposition amplitude (nm)	Slit-size (mm)	Amplitude uncertainty (nm)	Angular resolution (arcsec)
1	300	5	± 0	3.6
			± 10	3.6
			± 50	7.3
2	40	2	± 0	0.6
			± 1	1.0
			± 5	2.0
			± 10	3.5
3	4	1	± 0	0.2
			± 0.5	0.2
			± 1	0.5
			± 2	0.8

As discussed earlier, the contact-stylus profilometer used on the small-animal-imaging test optics had a limitation of around +/- 20 nm, whereas the best profilometers currently available at MSFC will achieve +/- 5 nm. The current state-of-the-art is +/- 1.5 nm; if this were implemented on these particular optics they would be improved from 6.8 arcsec to about 0.5 arcsec.

We have also included in our modeling uncertainties in shell registration, deposition rate and beam profile. We find that even for the highest stages of correction, their effects do not dominate. For example, standard machine-tolerance accuracies in mask dimensions and positioning are adequate for 0.2-arcsec-level ultimate resolutions. Note that the modeling above assumed that the shell figure errors were circumferentially symmetric and thus that all meridians could be corrected the same way. In practice there will be some variations around the shell. These circumferential variations, however, can be dealt with if necessary by using slits of limited azimuthal extent, and then rotating the shell around the mask with variable velocity

to vary the coating thickness around the shell as well as along it. In this way, the full inside surface of the shell would be corrected given adequate metrology.

Although the above discussion has concentrated on full-shell optics, of the type fabricated at MSFC, the technique will work equally well with segmented optics with a straightforward change of coating geometry. Given a 2-D topographical map of the surface to be corrected, a 2-D Gaussian beam can be scanned over the surface at variable velocity to effect the correction. As with the full shell optics, successively finer beams can be used improve the figure correction. Further, the segmented optics lend themselves readily to corrections while fully mounted, making this task easier than with full-shell optics. We intend, in the proposed study, to concentrate mainly on the application of differential deposition to the segmented mirrors currently being developed for an IXO-like mission, but will also investigate improvements that can be accomplished on full-shell replicated optics.

3. Proposed Work

We propose to develop a differential deposition system to improve significantly the angular resolution for astronomical optics, both segmented and full shell. To accomplish this we will construct a flexible coating system that will permit sputtering for each type of optic. It will incorporate various computer-controlled translation and rotation stages, with encoder readout to move masks and optics as appropriate. For full shells, we will use a concentric target rod; for large-diameter segmented optics, a suitably-sized planar target will be used (see Figure 3). The overall system will be configured for eventual incorporation of an in-situ metrology system, currently being developed at MSFC, which is designed to provide rapid measurements of substrates through the use of multiple beams and sensors.

When the deposition system is constructed, we shall fully characterize the coating parameters to obtain conditions (sputtering material, power levels, inert gas type and pressure) that give the best coating rates and high-quality deposits (low surface roughness, good adhesion and low stress) at appropriate substrate distances for each optic type. As necessary, we shall examine and quantify trades between these different parameters. For these tests, we shall use glass slides to measure coating thickness and adhesion, and superpolished silicon wafers to gauge the coating roughness. Deposition stresses will be assessed by measuring the degree of bowing in coated, thin silicon wafers.

For segmented optics, which we will at first approximate with simple glass flats, we shall investigate, initially through modeling, the use of large-slit masks to quickly fill in the larger features, possibly multiple areas simultaneously. We shall then investigate optimum approaches for finer-scale corrections. This could possibly entail slits with variable/commandable sizes under computer control and/or custom masks for each optic to be corrected

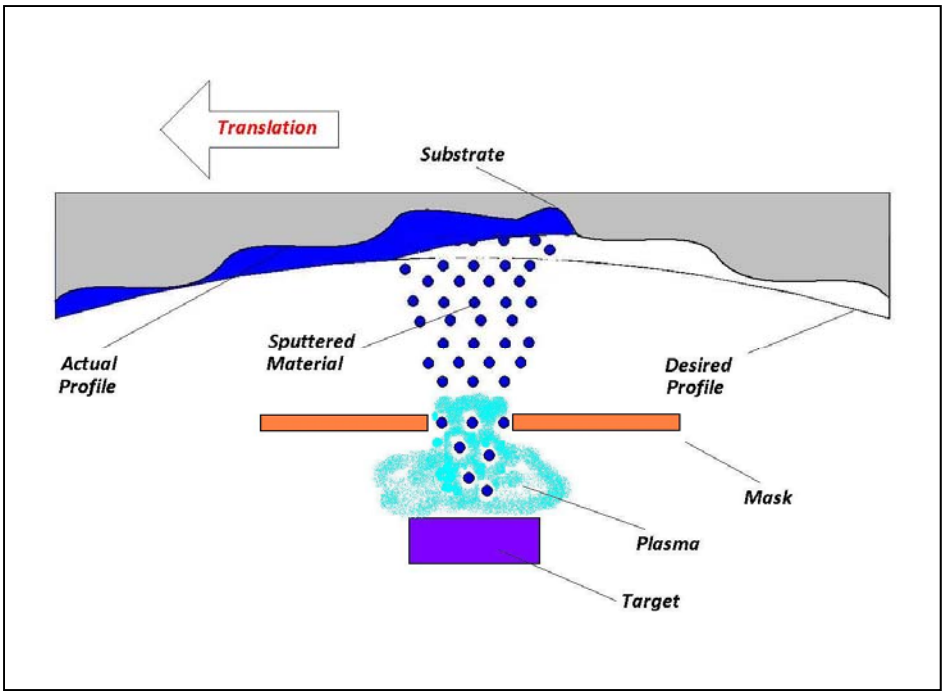

Figure 3: *Schematic of planar coating geometry for correcting segmented optics.*

As with the full-shell cylindrical optics evaluated to date, computer simulations will guide the correction approach, which will then be validated through mirror coatings and subsequent metrology. Additional effects, such as the change in beam profile and coating rate with (changing) substrate distance, will be modeled and verified by measurements, and the overall effect of these on the ultimate resolution will be assessed. A key issue for segmented optic correction will be the amount of metrology necessary to determine the 2-D hit map with sufficient (spatial) accuracy for a desired figure correction, and this will be addressed during the early stages of the program with characterization of slumped-glass test mirrors supplied by our collaborator at the GSFC. We note that, in principal, one can do full-surface interferometric measurement very quickly for mirror segments, enabling the construction of a low-to-mid-frequency hit map relatively easily for both un-mounted and mounted mirrors.

For the full-shell optics we shall investigate the use of custom masks that could correct the full optic length simultaneously. We have modeled this and find that it is straight forward to design a mask with a slit that extends the full length of the optic, but of a varying width designed to match the desired profile. The shell to be corrected is then rotated around the mask and those regions with greater slit width receive larger amounts of coating than those areas where the slit is finer. Several such masks would be used with varying spatial scales for different stages of correction, as before. Each mask would need to be custom built for a particular shell, but could be easily fabricated.

For full-shell optics that have azimuthally varying figure distortion, and for which a single large mask cannot be used, we shall investigate using variable shell rotation speed, while the shell also translates axially (also at variable speed). In this manner, the thickness of the coating

can be varied over the full surface on the inside of the mirror shell. As with all these tests, the computer models will be used to derive the optimum slit sizes and velocity profiles.

For both segmented and full-shell-type optics, the initial tests will be evaluated simply by comparing metrology obtained before and after differential-deposition figure correction. The final proof, however, will be to verify that the performance of an optic has improved to the level expected. For this, selected optics will be fully characterized using the MSFC 100-m x-ray beamline before and after correction to verify the expected improvements.

4. References

[1] Ice, G.E., Chung, J.S., Tischler, J.Z., Lunt, A. And Assoufid, L. 2000, **Rev. Sci. Instr**, 71(7) 2635-2639.

[2] Alcock, S.G. and Cockerton, S. 2010, **Nucl. Instr. & Meth. in Phys. Res.** A 616, 110-114.

[3] Kilaru, K, Ramsey, B.D., Gubarev, M.V. and Gregory, D.A. 2011, **Opt. Eng.** 50, 106501.

[4] Zhang, W. W. et. al. 2008, Proc. **SPIE**, 7011, 103.

[5] Kilaru, K., 'An Investigation of Differential Deposition for Figure Correction in Grazing Incidence Optics', Ph.D. Thesis, University of Alabama in Huntsville, 2010.

5. ROM Budget (all in ($k))

Element	Yr 1	Yr 2	Yr 3
Equipment *	245.0	42.5	25.0
CS labor +	1.0 FTE	1.5 FTE	1.5 FTE
Contractor labor +	35.0	125.0	140.0
Facility charges	29.0	50.0	60.0
Total procurement	309	217.5	225
Total CS labor	1.0 FTE	1.5 FTE	1.5 FTE

***** *Equipment costs based on actual quotes for coating chambers, sputtering power supplies, stages, pumps, gauges, etc.*

+ Labor estimates based on past coating, modeling and metrology activities.